

Dynamics of fire plumes and smoke clouds associated with peat and deforestation fires in Indonesia

M. G. Tosca,¹ J. T. Randerson,¹ C. S. Zender,¹ D. L. Nelson,² D. J. Diner,² and J. A. Logan³

Received 6 October 2010; revised 18 January 2011; accepted 27 January 2011; published 22 April 2011.

[1] During the dry season, anthropogenic fires in tropical forests and peatlands of equatorial Asia produce regionally expansive smoke clouds that have important effects on atmospheric radiation and air quality. Here we estimated the height of smoke on Borneo and Sumatra and characterized its sensitivity to El Niño and regional drought. We used Multiangle Imaging Spectroradiometer (MISR) satellite data and the MISR Interactive Explorer (MINX) software to estimate the heights of 317 smoke plumes on Borneo and 139 plumes on Sumatra during 2001–2009. In addition, we estimated the altitudes of larger smoke regions (smoke clouds) over Borneo using data from MISR and Cloud-Aerosol Lidar and Infrared Pathfinder Satellite Observation (CALIPSO) products. Most smoke plumes on Borneo (83%) were observed during El Niño years. Annually averaged plume heights on Borneo were significantly higher during El Niño events. Mean MISR-derived plume heights were 709 ± 14 m on Borneo and 749 ± 24 m on Sumatra during 2001–2009, with 96% of all plumes confined to within 500 m of the atmospheric boundary layer. Smoke clouds on Borneo were observed at altitudes between 1000 and 2000 m as measured by both MISR and CALIPSO. The difference in height between individual plumes and longer-lived regional smoke clouds may be related to deeper planetary boundary layers and higher-intensity fires later in the afternoon or other atmospheric mixing processes that occur on synoptic time scales. Our measurements and analyses suggested that direct injection of smoke into the free troposphere within fire plumes was not an important mechanism for vertical mixing of aerosols in equatorial Asia.

Citation: Tosca, M. G., J. T. Randerson, C. S. Zender, D. L. Nelson, D. J. Diner, and J. A. Logan (2011), Dynamics of fire plumes and smoke clouds associated with peat and deforestation fires in Indonesia, *J. Geophys. Res.*, 116, D08207, doi:10.1029/2010JD015148.

1. Introduction

[2] Peat and deforestation fires in Indonesia occur more frequently during El Niño droughts, when farmers take advantage of drier fuels and lower water tables to convert natural ecosystems to agriculture [Page *et al.*, 2002; Field *et al.*, 2009]. Deliberate ignition is used to clear land for pulp and timber plantations, transmigrant settlements, roads, and oil palm plantations, the latter of which tripled in number between 1985 and 1997 [Aiken, 2004; Murdiyoso and Adiningsih, 2007]. Over time, widespread fragmentation and degradation have exacerbated the susceptibility of Indonesia's forests to fire [Aiken, 2004]. These large-scale anthropogenic fires disrupt ecosystems and biodiversity

[Sodhi *et al.*, 2004] and influence regional air quality and climate through aerosol emissions [Davies and Unam, 1999; Tosca *et al.*, 2010]. During the 1997/1998 El Niño nearly one third of global fire emissions originated from Indonesia, an amount approximately equal to 0.8–1.0 Pg C [Page *et al.*, 2002; van der Werf *et al.*, 2006, 2008]. Integrating over both El Niño and La Niña periods, emissions associated with peat and deforestation fires are similar in magnitude to fossil fuel emissions from the region. For example, during 2000–2006 mean fire emissions from Indonesia were 128 Tg C yr^{-1} [van der Werf *et al.*, 2008], compared to 141 Tg C yr^{-1} from fossil fuel emissions [Marland *et al.*, 2006; Boden *et al.*, 2010].

[3] Trace gases and aerosols emitted from Indonesian fires have important consequences for regional atmospheric chemistry, air quality and climate, providing motivation here for our investigation of the temporal and spatial dynamics of smoke plumes and clouds. Emission and transport of carbon monoxide (CO), nitrogen oxides, and volatile organic compounds from these fires increase levels of tropospheric ozone across large areas of Southeast Asia and the Indian Ocean [Thompson *et al.*, 2001; Duncan *et al.*, 2003; Logan

¹Department of Earth System Science, University of California, Irvine, California, USA.

²Jet Propulsion Laboratory, California Institute of Technology, Pasadena, California, USA.

³School of Engineering and Applied Science, Harvard University, Cambridge, Massachusetts, USA.

et al., 2008]. Smoke from these fires also contains high levels of particulate matter with diameters less than 10 μm (PM_{10}) [e.g., *Andreae and Merlet*, 2001]. In the city of Kuching on the island of Borneo, for example, atmospheric concentrations of PM_{10} were ~ 20 times higher than normal levels during the fall of 1997, reducing visibility to 50 m during severe haze episodes [*Davies and Unam*, 1999]. PM_{10} concentrations in Singapore were 3 times higher than normal during this time and caused substantial increases in upper respiratory illnesses, asthma and rhinitis [*Emmanuel*, 2000]. Airport visibility records across Sumatra and Borneo indicate that reductions in air quality from fires during the 1997/1998 El Niño were probably the largest observed in equatorial Asia during the last four decades [*Field et al.*, 2009].

[4] In addition to impacts on chemistry and air quality, smoke aerosols reduce surface radiation, increase atmospheric absorption, and modify cloud microphysics, the combination of which may change precipitation patterns in equatorial Asia. *Podgorny et al.* [2003] observed a reduction in mean surface insolation of 20–30 W m^{-2} over much of the tropical Indian Ocean and Indonesia during the large smoke events of 1997. *Duncan et al.* [2003] estimated similar reductions in surface radiation, including a maximum decrease of over 170 W m^{-2} in insolation across Indonesia. Investigating the effect of these aerosols on regional climate using the Community Atmosphere Model (CAM), *Tosca et al.* [2010] found significant reductions in precipitation (by approximately 10%–15% over Sumatra and Borneo) in response to fire-emitted aerosols during moderate El Niño periods. These reductions in precipitation occurred as a consequence of aerosol-induced heating of the midtroposphere and concurrent reductions in land and ocean surface temperatures that suppressed convection near aerosol source regions. Other dynamical responses to smoke aerosols are expected. *Ott et al.* [2010] show, for example, that increased cloudiness over Indonesia likely occurred in response to aerosols emitted during the 2006 El Niño.

[5] Current atmospheric chemical transport models (CTMs) often require smoke injection heights as inputs [e.g., *Westphal and Toon*, 1991; *Colarco et al.*, 2004]. In the standard version of GEOS-Chem, for example, fire aerosols are distributed within the boundary layer. This is probably adequate for small fires and for those that have a large smoldering phase or are of low intensity. However, in many ecosystems fire plumes have been observed in the mid and upper troposphere [e.g., *Andreae et al.*, 2001; *Fromm and Servranckx*, 2003]. The frequency of these events and their importance for atmospheric chemistry and radiation as well as for inverse studies of sources and sinks of greenhouse gases remains uncertain and is an area of active research.

[6] Several groups have investigated the impact of smoke plume injections on regional and global patterns of atmospheric trace gases and aerosols. *Freitas et al.* [2006] developed a prognostic approach for simulating plume heights that accounted for buoyancy using the energy flux and area of each fire. Using this plume model, the authors show that accounting for injection processes can improve regional atmospheric model predictions of tropospheric CO across the central Amazon as compared with Atmospheric Infrared

Sounder (AIRS) and aircraft observations. In boreal regions, injection of fire emissions above the boundary layer in models also can improve agreement with CO observations [*Leung et al.*, 2007; *Chen et al.*, 2009]. A key challenge that remains with respect to representing plume injections in atmospheric models is to develop realistic parameterizations that are internally consistent with remote sensing-derived estimates of plume heights, burned area, and rates of fuel consumption. An important and sometimes overlooked step during model evaluation is to ensure injection processes are not compensating for other errors within the atmospheric model, including, for example, biases the strength of convective mixing within the free troposphere [e.g., *Yang et al.*, 2007].

[7] Recent remote sensing advances provide a means for systematically evaluating smoke injection heights and transport processes that mix these aerosols within troposphere [e.g., *Labonne et al.*, 2007; *Kahn et al.*, 2008; *Val Martin et al.*, 2010; *Mims et al.*, 2010]. Smoke heights may be obtained using either spaceborne lidar or stereo imaging, with the former providing information about the vertical structure of aerosols within smoke clouds and the latter offering vastly greater horizontal coverage [*Kahn et al.*, 2008]. Both approaches allow for detection of the heights of plumes (smoke with a discernable surface origin) and smoke clouds (smoke with no detectable origin). *Labonne et al.* [2007] investigated smoke aerosol heights using the Cloud-Aerosol Lidar with Orthogonal Polarization (CALIOP) product, flying on board the Cloud-Aerosol Lidar Infrared Pathfinder Satellite Observation (CALIPSO) satellite. Their study of several hundred globally distributed cases provides evidence that smoke is confined mostly to the atmospheric boundary layer (ABL). An alternate approach taken by *Kahn et al.* [2008] used stereo-derived plume heights from the Multiangle Imaging Spectroradiometer (MISR) to show that approximately 5% of boreal smoke plumes in the Alaska-Yukon region during the summer of 2004 had median heights that were more than 500 m above the ABL. These findings are consistent with earlier work documenting isolated cases where smoke was injected into the free troposphere [e.g., *Fromm and Servranckx*, 2003]. In a comprehensive survey, *Val Martin et al.* [2010] analyzed 3367 plumes across North America during 2002 and 2004–2007. Their analysis indicates that that approximately 4%–12% of North American plumes have median heights exceeding 500 m above the top of the ABL and that plume heights vary significantly as a function of biome type. Smoke plumes from areas in southern Mexico dominated by subtropical forests and agriculture have median heights that are among the lowest of all North American biomes, and are the least likely to occur above the ABL [*Val Martin et al.*, 2010]. Temperate and boreal plumes are more likely to be injected above the ABL. For plumes that rise above the ABL, more than 80% become trapped within a stable layer.

[8] *Val Martin et al.* [2010] also find that smoke clouds occur more often above the ABL at altitudes exceeding those of nearby smoke plumes. Approximately 35% of smoke clouds have heights that are more than 500 m above the ABL. This suggests that vertical transport processes play a key role in the evolution of plumes into clouds. The authors suggest that some of this height differential can be

explained by increased afternoon fire intensities that elevate smoke from younger plumes earlier in the day. In addition, they note that atmospheric advection processes unrelated to fire also may transport smoke to higher altitudes.

[9] Here we estimated fire smoke heights on the islands of Borneo and Sumatra during 2001–2009 using satellite observations from MISR and CALIPSO. We analyzed both plumes (smoke with a visible surface source and transport direction) and clouds (dispersed smoke that was opaque but with no discernable surface source) from MISR observations. We independently assessed smoke cloud heights using CALIPSO observations. We analyzed differences in heights and horizontal coverage between regional smoke clouds and individual smoke plumes. We also analyzed temporal and spatial patterns of plumes as well as links between El Niño and plume height.

2. Methods

[10] In this manuscript we used satellite imagery to characterize the structure of biomass burning smoke features over Borneo and Sumatra. We determined the height, shape, seasonality and geographical distribution of smoke using data from MISR and CALIPSO. A map of terrestrial ecosystems from the World Wildlife Fund (WWF) was used to identify the location of plumes originating from peat forests on the islands. We also compared the temporal distribution of smoke plumes with active fire observations from MODIS.

2.1. MISR Smoke Plume and Cloud Height Retrievals

[11] The MISR instrument, on board the Terra satellite, measures surface and atmospheric properties with nine cameras, each at a different angle in line with the ground track of the satellite [Diner *et al.*, 1998]. Fire smoke altitudes were obtained from stereo-derived altitude estimates using the MISR Interactive Explorer (MINX) software [Nelson *et al.*, 2008a, 2008b]. Using MINX, the origin, perimeter and transport direction of each plume are user determined and are manually digitized via an interactive user interface. MINX automatically computes zero-wind and wind-corrected feature altitude estimates using a forward modeling technique that combines retrieval results from up to six camera pairs, each using the nadir camera as reference.

[12] In this manuscript, we refer to smoke features with identifiable surface origins as “plumes” and regions of dispersed smoke not associated with a source point as “clouds.” Plumes are generally narrower, less opaque, and exhibit a visible direction of transport from their origin. Although smoke clouds may persist for several days, individual MISR images from different days were treated as independent measurements for our estimates of cloud altitudes and smoke spatial extent, as reported below.

[13] We identified all visible plumes from January 2001 through December 2009 on the islands of Borneo and Sumatra. It would have been prohibitively time intensive to manually inspect the large number of available MISR orbits to find these smoke plumes. Instead we used a MINX utility to identify and retrieve only those MISR scenes that contained MODIS (MOD14A2) active fires [Giglio *et al.*, 2006]. Since the MODIS instrument on the Terra satellite

images every scene that MISR observes, only those MISR scenes containing MODIS active fire pixels were analyzed.

[14] MISR scenes were selected for inclusion in the study if they contained at least one MODIS active fire pixel. Within a scene, plumes were accepted for inclusion if they exhibited substantial opacity, had a clearly defined transport direction, and were not obscured by water clouds. Most plume origins were located near a MODIS active fire pixel, but plumes within a scene not originating from a MODIS active fire pixel also were digitized as long as they met the other criteria described below. Each plume’s source, perimeter, transport direction and association with one or more MODIS active fire pixels were identified by visual inspection and were manually digitized by the user (M. Tosca). In a second step, the plume database was reviewed by a second user (D. Nelson). Of the initial plumes, 18% were redrawn, 13% were deleted, and 2% were added.

[15] The MINX algorithm estimates both zero-wind and wind-corrected altitudes. The zero-wind calculation assumes that all the apparent camera-to-camera motion of a plume or cloud in the spacecraft’s ground track direction is due to parallax. This parallax effect is proportional to the height of the feature above the terrain, so the height is easily retrieved. However, in the presence of wind that has a component in the ground track direction, there is additional motion that must be separated out. The wind correction performs this separation and reports only the true altitude due to parallax.

[16] Wind-corrected stereo altitudes are therefore more accurate [Kahn *et al.*, 2007] and were used in the analysis presented below. We refer to the “height” of each retrieval as the difference between the wind-corrected smoke top altitude and the terrain altitude, both determined by MINX. Smoke clouds, by our definition, have no visual characteristics that can be used to identify their direction of transport. Therefore, no directional information was specified for them during digitizing, and we report the zero-wind heights for our MISR smoke cloud analysis. Although all plumes and clouds were carefully screened, manual digitization may introduce biases, including, for example, the inclusion of nonsmoke features within the digitized feature perimeter and operator-defined estimates of plume length. Careful consideration was made to remove all potential water cloud contamination, during both the manual digitization phase and the postprocessing screening phase. Water clouds were generally higher and brighter than smoke clouds and were therefore easily identified for removal. Stereoheights for thin plumes were generally of low quality, and often height retrievals for these plumes comprised a smaller percentage of the total area within the digitized perimeter than for thicker plumes. Poor quality plumes were defined as those that were not composed of at least five valid height retrievals or those that contained water cloud contamination. If water clouds could be removed from the original plume perimeter, the plume was redigitized, otherwise these and other poor quality plumes were excluded from our analysis.

[17] The total sample size of high-quality plumes observed in this study was 456, with 317 on Borneo and 139 on Sumatra. Many more plumes were visible, but were too thin or too small to digitize. In addition, in many cases more than one active fire detection occurred near the plume origin. Many other active fires did not have distinct plumes

associated with them. As a result of these factors, the number of MODIS active fires observed over Borneo and Sumatra (148519) was several orders of magnitude larger than the number of digitized smoke plumes (456). The number of plumes for each of the 9 years varied greatly, from 2 plumes in 2008 to 153 in 2006. As described below, much of this variability was a result of increased fire activity during years with El Niño-induced drought.

[18] Terrain altitudes for plume origins from MINX were positively correlated with an independently derived digital elevation model from NOAA ($r = 0.5$; Figure S1 in the auxiliary material) [Hastings *et al.*, 1999], though MINX terrain estimates did show a small positive mean bias of 34 m.¹ Plume altitudes refer to the height of smoke above sea level. Plume heights for individual plumes were calculated as the mean of all individual pixel retrieval heights within the digitized perimeter. Annual mean plume height for the region was calculated as the mean height of the individual plumes. We used standard errors (the standard deviation (σ) divided by the square root of the number of observations (n)) to define sampling uncertainties for plumes in our results. Because smoke clouds contained too many retrievals to present a reasonable standard error, we report straight standard deviations for that data.

[19] We used a two-step transformation to create a representation of the mean plume shape for all smoke plumes on Borneo. We translated each plume to a common origin and then rotated all plumes to a common downwind direction defined by each plume's centroid.

[20] Using MINX, we also digitized all visible smoke clouds near or over the island of Borneo during the fall of 2006. We focused on this period for our more detailed analysis because it had the highest number of fire plumes (and MODIS active fire counts) measured during our 9 year study period. Ten smoke clouds were digitized between 26 September 2006 and 30 October 2006. We calculated smoke cloud altitudes as the mean height above sea level of all individual cloud retrievals. The total mean smoke cloud altitude for 2006 was the mean of all individual smoke retrievals. Individual smoke plume altitudes were also estimated to allow for a direct comparison with MISR smoke clouds.

2.2. CALIPSO Altitude Retrievals

[21] We analyzed all available day and night CALIPSO observations within 3°S–3°N and 110°E–117°E (over the island of Borneo) from the beginning of the CALIPSO record on 1 July 2006 through 31 December 2009. We retrieved smoke layer top altitudes for each overpass from the CALIPSO Lidar Level 2 5 km aerosol product (CAL_LID_L2_05kmALay-Prov-V3-01). We also retrieved vertical aerosol extinction coefficient data from the product CAL_LID_L2_05kmAPro-Prov-V3-01. Smoke aerosols are distinguished within the CALIPSO backscatter data using an algorithm developed by Omar *et al.* [2009]. The algorithm first estimates the aerosol extinction-to-backscatter ratio (S_a) and then passes S_a through an extinction retrieval algorithm,

developed by Young and Vaughan [2009]. Once the feature is distinguished as smoke, a separate algorithm determines an array of threshold values for smoke (at varying vertical levels), obtains a profile of attenuated scattering ratios from the raw backscatter data and then scans a prescribed range of altitudes from top to bottom until the attenuated scattering ratio exceeds the threshold value [Vaughan *et al.*, 2005]. Smoke layer top altitudes are available at a 5 km horizontal (and varying vertical) resolution. For each CALIPSO scene we constructed a time series of the 16 day mean along-track, one-dimensional fractional coverage of smoke aerosols. To verify the associations between El Niño, precipitation and fire occurrence, we compared the CALIPSO time series of smoke fractional coverage with a 16 day mean precipitation time series derived from the Tropical Rain Measuring Mission (TRMM) 3B42 version 6 product. This precipitation time series had a daily time step and a $0.25^\circ \times 0.25^\circ$ spatial resolution [Kummerow *et al.*, 1998]. For analysis of smoke altitudes we used only CALIPSO overpasses that contained 15% or more horizontal smoke coverage within our study region.

2.3. Atmospheric Boundary Layer Retrievals

[22] We used ABL heights from the NASA Global Modeling and Assimilation Office (GMAO) Modern Era Retrospective-Analysis for Research and Applications (MERRA) reanalysis product [Bosilovich *et al.*, 2008]. ABL data from MERRA was derived from the Goddard Earth Observing System, version 5 (GEOS-5) reanalysis product and had a spatial resolution of $0.5^\circ \times 0.66^\circ$ and 1 h temporal resolution. We obtained all ABL heights from 2001 to 2009 at 1100 local time (LT), and computed each year's fire season ABL height for southern Borneo as the mean of all estimates between 4°S–0° and 109°E–118°E for 1 July through 31 October. Plumes were considered above the ABL if their mean heights were 500 m or more above the top of the MERRA-derived ABL for the same day at each grid cell.

2.4. Spatial Distribution of Peat Forests

[23] We used the World Wildlife Fund (WWF) terrestrial ecoregions map [Olson *et al.*, 2001] to identify areas with peat forests on Sumatra and Borneo. We created an aggregate vegetation class as the combination of peat swamp (class numbers 40104 and 40160), freshwater swamp (class numbers 40153 and 40157) and heath forest (class number 40161) ecoregions. All of these ecoregions had similar peat soil surface layers and plant species [Wikramanayake *et al.*, 2001]. This aggregate vegetation class was mostly located in southern Borneo and eastern Sumatra. We used ArcGIS software to regrid the WWF vector data to a $0.1^\circ \times 0.1^\circ$ spatial resolution raster map.

2.5. Active Fires

[24] We used the Level 3 tile-based (1 km) 8 day composite of active fires from Terra (MOD14A2) [Giglio *et al.*, 2006; <http://modis-fire.umd.edu/>] to determine which MISR scenes contained smoke suitable for digitization. We used the coarser resolution (0.5°) 8 day Climate Modeling Grid (CMG) MODIS active fire product (MOD14C8H) to compare large-scale spatial and temporal distributions of smoke

¹Auxiliary materials are available in the HTML. doi:10.1029/2010JD015148.

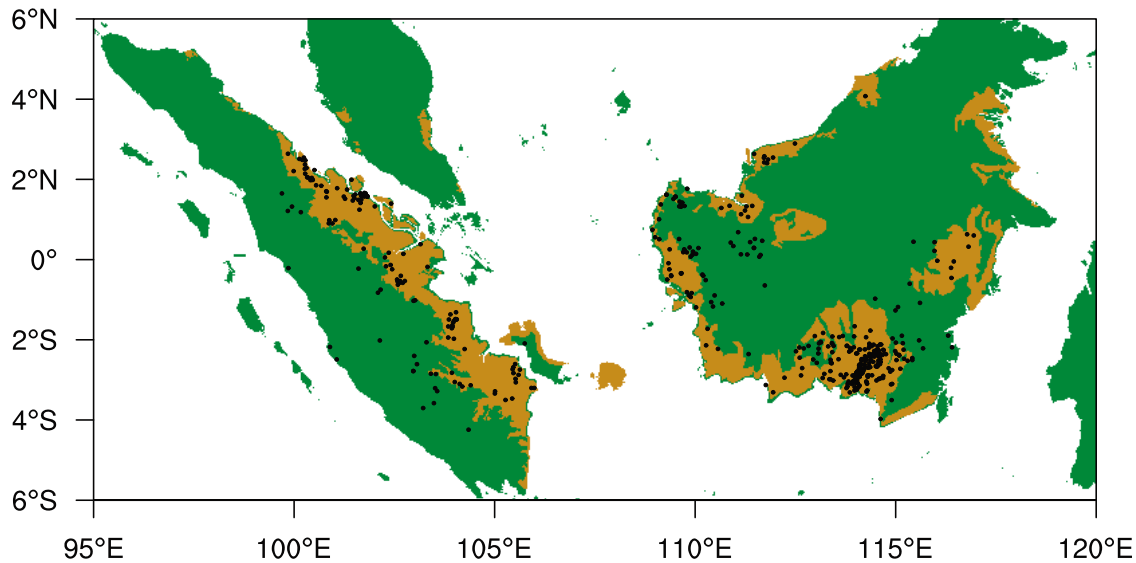


Figure 1. Location of plumes on Borneo and Sumatra digitized in this study (black dots). Brown regions indicate peat forests (peat, freshwater swamp, and heath forest ecoregions); green regions are other forest and nonforest ecoregions.

plumes with active fires. This product had an 8 day time step and included corrections for gaps in satellite coverage. Finally, we used the Level 2 (daily) 1 km gridded composite of fire pixels from both Aqua (MYD14A1) and Terra (MYD14A1) to determine the total number of active fires in peat forests.

3. Results

3.1. Smoke Plumes Originating From Peat Forests

[25] We observed 456 plumes on Borneo and Sumatra during 2001–2009, most of which originated from fires in peat forests (Figure 1 and Table 1). The year-to-year fraction of plumes observed in peat forests was negatively correlated with the Oceanic Niño Index (ONI), an indicator of El Niño (Figure S2a). In contrast, the fraction of active fires in peat forests was positively correlated with ONI (Figure S2b). Plume heights in peat forests and nonpeat regions were similar: 700 ± 13 m versus 727 ± 13 m, respectively.

3.2. Plume Injection Heights

[26] Most of the 317 plumes on Borneo were observed between August and October (Figure 2a). Reasonable agreement between the 8 day average of the number of MISR plumes and MODIS CMG active fires suggested that seasonal patterns in the number of digitized plumes were consistent with the seasonal distribution of active fire detections. Precipitation was a primary driver of the considerable interannual variability of plume number and active fires during the dry season (Figure 3a). Borneo precipitation during August–October for 2002, 2004, 2006 and 2009 averaged 27% (1.6 mm d^{-1}) below the 2001–2009 August–October mean. These years accounted for 83% of all plumes and 77% of all fire counts observed during 2001–2009.

[27] Most plume retrievals were observed south of the equator and between 112°E and 116°E , primarily within the

Central Kalimantan province of Indonesia (Figures 1 and 4a). A smaller cluster of plumes was observed west of 112°E and between 1°S and 3°N in West Kalimantan province and far southwest Sarawak province in Malaysia. Several isolated plumes were also detected in East Kalimantan province. Plume heights from Borneo did not show any significant differences across these different provinces (Figure 4b). For reasons described in section 2.1, there were substantially more active fire pixels than smoke plumes (Figure 4c). MODIS (CMG) fire radiative power (FRP) was fairly uniform throughout the region, with local maxima in southern and western Borneo (Figure 4d).

[28] The mean height of all plumes on Borneo was 709 ± 14 m (Figure 5a and Table 2). Plumes during dry years (associated with El Niño events) exhibited a statistically significant (99% confidence) higher mean height (724 ± 16 m) than plumes during wet years (633 ± 23 m). Dry years also were responsible for 100% of plumes that had mean heights extending more than 500 m above the top of the ABL. Mean plume heights were highest in 2002 (854 ± 44 m) when the June–November mean ONI reached its maximum value (1.2°C) of the 2001–2009 period. The Oceanic Niño Index is a measure of the 3 month average temperature anomaly in the Niño 3.4 region of the central Pacific (5°S – 5°N , 120°W – 170°W) [Trenberth, 1997]. Following the definition that an El Niño requires a minimum of five consecutive months of ONI greater than 0.5°C , four

Table 1. Distribution of Plumes and Active Fires in Peat Forests

	Peat Forests	“Other” Ecoregions
Plumes (number)	342	114
Plumes (%)	75	25
Active fires (%)	62	38
Plume height (m)	700 ± 13	727 ± 26

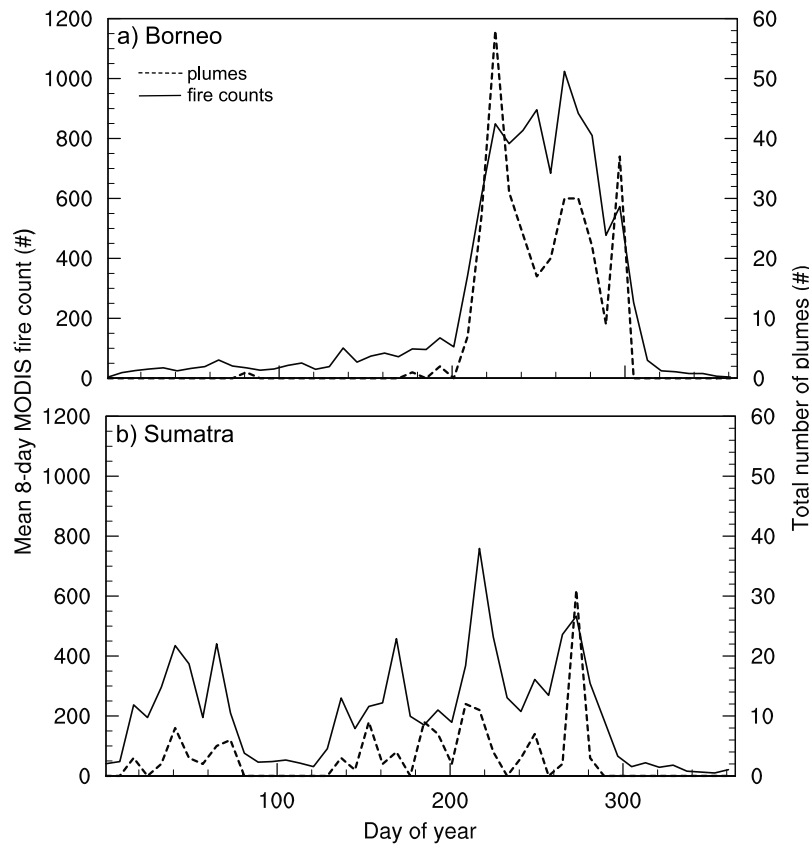


Figure 2. Seasonal distribution of the number of observed (MODIS CMG) active fires (solid line) and the number of observed (MISR) smoke plumes (dashed line) for (a) Borneo and (b) Sumatra. These distributions are the annual means during 2001–2009.

years during 2001–2009 met this criterion: 2002, 2004, 2006, and 2009.

[29] Annually averaged ABL heights (from MERRA reanalysis) and mean fire radiative power (from MODIS CMG) for the region were both positively correlated with ONI ($r^2 = 0.7$ for both), suggesting that the higher plumes during El Niño events were partly a result of higher ABL heights and hotter fires (Figures 6a and 6b). Weighting for the number of observed plumes each year (2001–2009, and excluding 2008 for which we only measured 1 plume), we observed a weak positive correlation between observed plume height and ONI ($r^2 = 0.4$; Figure 6c). Monthly MERRA ABL height anomalies and ONI were significantly correlated during 2001–2009 (Figure S3). Annual mean plume height also was weakly correlated with ABL ($r^2 = 0.3$) but not FRP. Additionally, individual plumes were not correlated with their corresponding FRP or ABL.

[30] Unlike Borneo, plume occurrence on Sumatra was more evenly distributed throughout the year, with two discernable periods of fire activity. The first burning season spanned from January–April, and the second corresponded to a summer/fall period (May–November) similar to the one observed on Borneo (Figure 2b). MODIS active fires indicated that the first burning season on Sumatra was most pronounced in the north (Riau province) (Figure S4).

[31] A majority of the 139 identified Sumatran plumes were observed on the east coast of the island in Riau, Jambi and South Sumatra provinces (Figures 1 and 4a). MODIS (CMG) fire counts also were concentrated in these provinces (Figure 4c). Mean FRP was more uniform, with local maxima along the eastern Sumatran coast (Figure 4d). Sumatra plume heights had a mean of 749 ± 24 m (Figures 4b and 5b and Table 2), similar to those on Borneo. The mean height of all plume retrievals from the January–April burning season was similar to the mean height of plume retrievals during May–November (e.g., Table 2 and Figure 5b).

3.3. Indonesian Smoke Cloud Altitudes From MISR During 2006

[32] We identified 10 smoke clouds from MISR observations over Borneo during the fire season of 2006 (26 September to 30 October 2006). Smoke clouds during this period of intense burning (e.g., Figure 3) were spatially expansive, highly visible and easily digitized. Smoke clouds had mean altitudes (and standard deviations) ranging from 1064 ± 431 to 1795 ± 456 m (Table 3 and Figure S5). Weighted by the total number of smoke retrievals within each cloud, the mean altitude of all 2006 smoke clouds was 1375 ± 608 m, compared with 836 ± 110 m for all 2006 Borneo individual plume retrievals (Figure 7). 95% of all plume retrievals had an altitude of 1370 m and below. For smoke clouds, this value

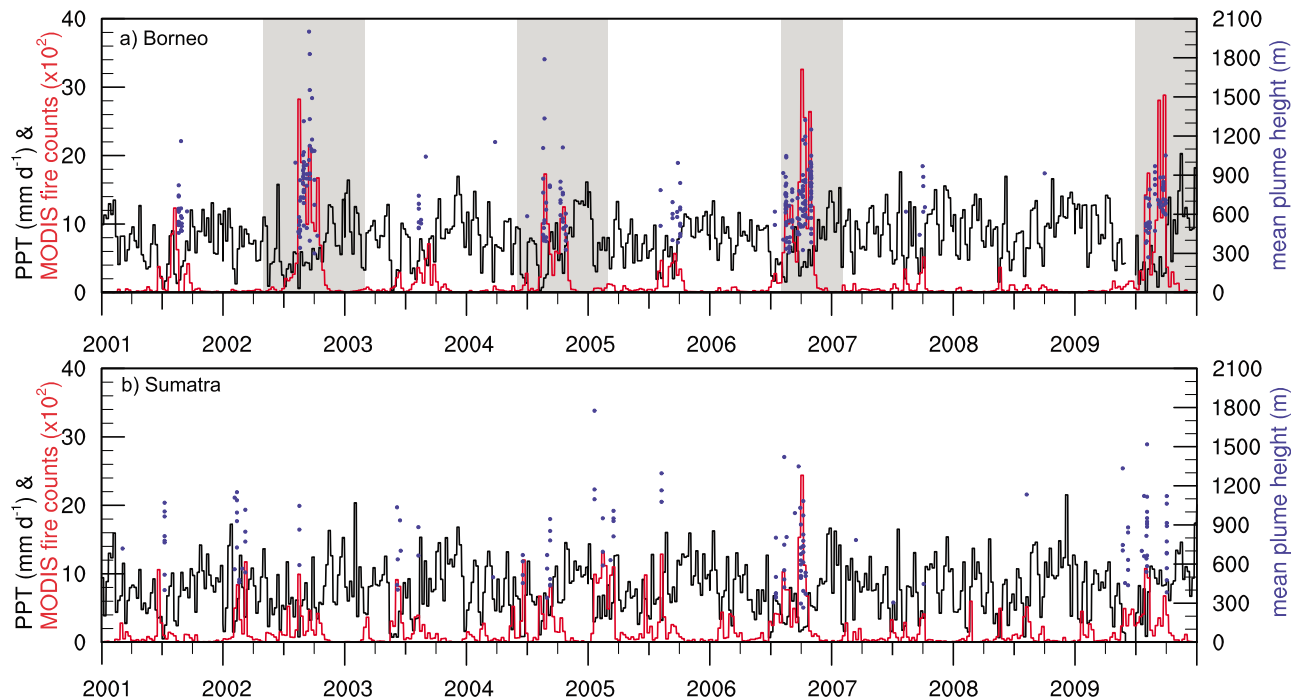


Figure 3. The 2001–2009 time series of 8 day MODIS CMG active fires (red; fire counts per 8 day period), 8 day average TRMM precipitation (black; mm d^{-1}), and the mean height of all individual fire plumes (blue dots; meters above terrain) for (a) Borneo and (b) Sumatra. Gray regions indicate periods of El Niño conditions in the eastern Pacific (defined by a sustained 5 month running mean Oceanic Niño Index greater than 0.5°C).

was over 1000 m higher (2378 m). Together, these statistics suggest that cloud altitudes were significantly higher and more variable than plume altitudes.

[33] Most of the smoke cloud retrievals were located over south-central Borneo (Figure S5), although several distinct clouds also were observed further west, over the ocean and over western provinces. Smoke clouds over the ocean had a lower mean altitude (1127 ± 588 m) compared to those over land (1441 ± 613 m). The smoke cloud observed on 12 October 2006 over south-central Borneo was the highest, with a mean altitude of 1795 ± 456 m and with over 33% of the individual smoke height retrievals having altitudes exceeding 2000 m.

3.4. CALIPSO Smoke Altitude Retrievals During 2006–2009

[34] We examined 806 daytime (~ 1300 LT overpass) and nighttime (~ 0100 LT overpass) CALIPSO tracks for 3°S – 3°N and 109°E – 118°E (over southern and central Borneo) between 1 July 2006 and 31 December 2009 (Figure S6). Smoke top altitudes, vertical aerosol extinction profiles and horizontal smoke fractional coverage were obtained from each overpass. Horizontal fractional smoke coverage and precipitation levels from TRMM were negatively correlated ($r = -0.7$ for day overpasses and $r = -0.6$ for night overpasses), providing more evidence that regional biomass burning substantially contributed to smoke observed over Borneo by CALIPSO (Figure 8a). The fraction of smoke cover was highest during the summer and fall of 2006

and 2009; this is consistent with the MODIS and MISR observations described in sections 3.1 and 3.2 that showed greater fire activity during moderate El Niño events (e.g., Figure 3).

[35] Mean smoke top altitudes generally ranged from 1000 to 6000 m above sea level for CALIPSO overpasses with 15% or higher horizontal smoke fractional coverage. However, the extinction-weighted mean altitudes for most overpasses were much lower, ranging from 500 to 4000 m above sea level (Figure 8b). There were a few scenes where the extinction-weighted mean aerosol altitudes were higher than their corresponding smoke top altitudes, and this appeared to be due to the presence of a small number of high-altitude, optically thick aerosol retrievals not associated with biomass burning smoke.

[36] Aerosol extinction data from the summer and fall fire season of 2006 showed smoke mostly confined between 500 and 2500 m above sea level with a 26 September to 31 October mean of 1643 ± 279 m for nighttime overpasses (e.g., Figure S7a). These altitudes were similar to the mean of MISR smoke cloud altitudes (1375 ± 192 m) for the same period. However, the Level 2 CALIPSO smoke top altitude product yielded values that were much higher and ranged between 2500 and 4000 m, with a mean of 3550 ± 161 m above sea level for night overpasses (Figure S7b). These top altitudes corresponded to mean extinction levels that were approximately seven times smaller than the maximum extinction coefficient observed for a 0.2 km vertical increment that was ~ 1200 m lower. The two instruments use

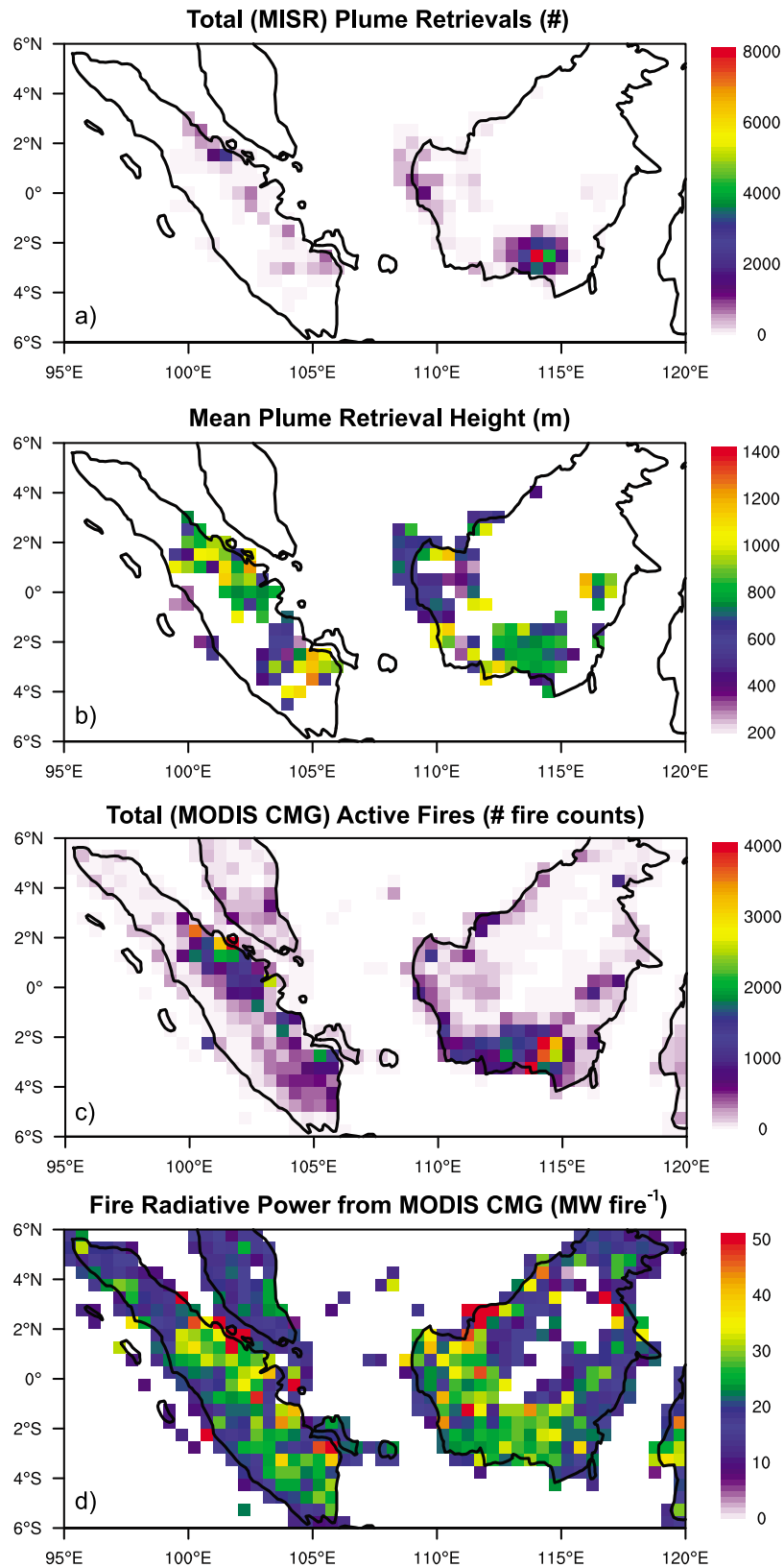


Figure 4. Maps showing the spatial distribution of plumes and active fires for Borneo and Sumatra during 2001–2009. (a) Active fires from the MODIS CMG product, (b) mean plume heights (meters above terrain), (c) total observed plume retrievals, and (d) mean fire radiative power (MW fire^{-1} ; from MODIS CMG). Plume information was averaged within each $0.5^\circ \times 0.5^\circ$ grid cell.

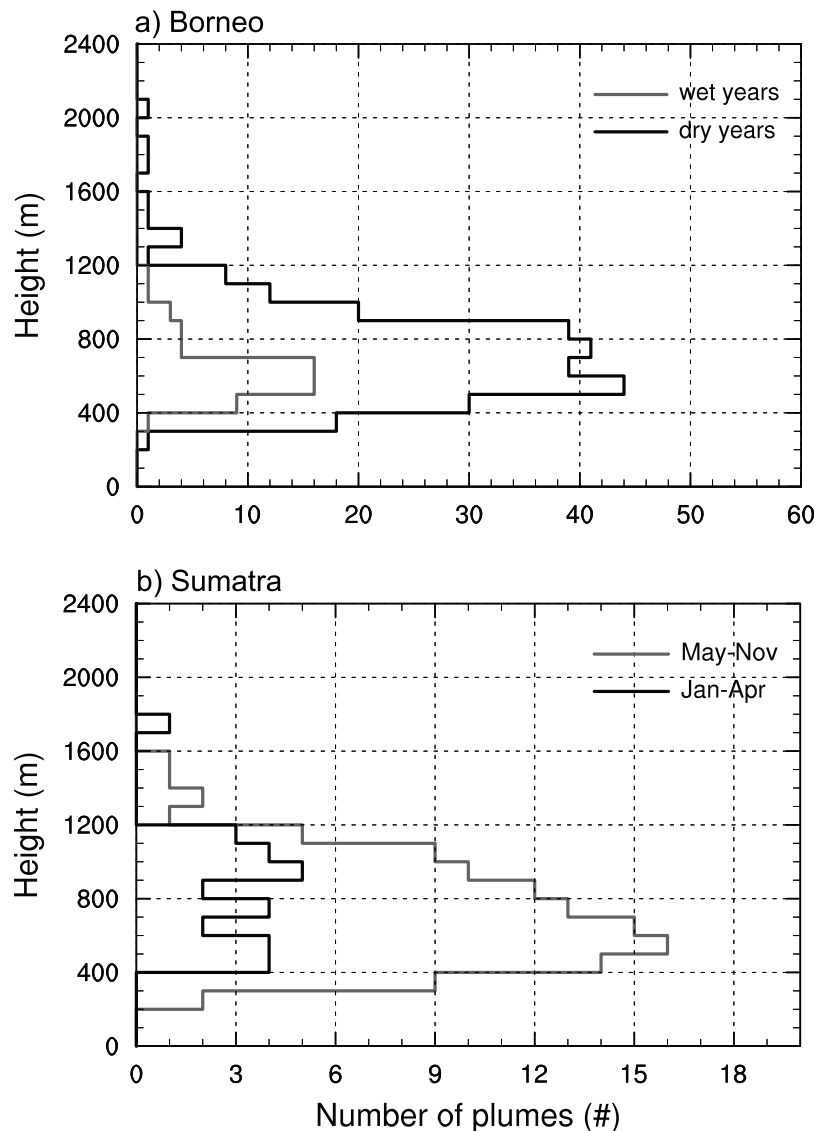


Figure 5. (a) Histogram of Borneo mean plume injection heights (meters above terrain) separated into dry year (years associated with El Niño; 2002, 2004, 2006, and 2009) and wet year (2001, 2003, 2005, 2007, and 2008) components. (b) Histogram of Sumatra mean plume injection heights (meters above terrain) separated into either a winter/spring (January–April) or summer/fall (May–November) burning season.

methods for determining height that can be expected to return different results. MINX uses a stereoscopic technique to retrieve heights by matching the red-band features in a scene between pairs of cameras, keying off layers of maximum spatial contrast [Nelson *et al.*, 2008a, 2008b]. This requires relatively opaque smoke over land to avoid matching on the terrain below. The CALIPSO lidar product for smoke top altitude, in contrast, appears to be triggered at far more diffuse (optically thin) aerosol layers that exist at higher altitudes. Analysis of the vertical cross section of aerosol extinction coefficients from fall 2006 shows that, while most smoke was observed between 1000 and 2000 m, the Level 2 CALIPSO product estimated a mean smoke top altitude above 3000 m (Figure S7b). Because CALIPSO retrieval is more sensitive to thin aerosol layers it is more likely to detect low-density smoke that has been raised by

turbulent mixing, air mass advection and, potentially by self-lofting. Therefore, the statistics presented here may hide details about plume evolution that can explain remaining differences between the two products.

3.5. Mean Direction, Shape, and Heights of Borneo Plumes

[37] Individual MISR-observed plumes on Borneo exhibited a very consistent transport direction and shape. Nearly all plumes drifted from southeast to northwest, with few plumes drifting in the opposite direction (Figure S8). We normalized each plume along its origin-to-centroid axis and found that the width of most plumes expanded slowly over the first 80 km as defined using a 2 sigma cutoff on the number of observations within 1 km increments along the centroid axis (Figures 9 and S9). Plume lengths were somewhat arbitrarily

Table 2. Summary of Fire and Plume Height Data for Borneo and Sumatra

Year ^a	Fire Count ^b	Number of Plumes	Mean Plume Height \pm SE ^c (m)
<i>Borneo</i>			
2001	5,065	21	618 \pm 37
2002	16,165	59	854 \pm 44
2003	4,488	9	636 \pm 58
2004	10,425	37	683 \pm 50
2005	4,424	17	599 \pm 39
2006	19,403	115	699 \pm 20
2007	2,676	7	715 \pm 69
2008	1,728	1	914
2009	14,664	51	662 \pm 23
All	79,038	317	709 \pm 14
“Dry”	60,657	262	724 \pm 16
“Wet”	18,381	55	633 \pm 23
<i>Sumatra</i>			
2001	3,508	9	782 \pm 73
2002	8,486	18	789 \pm 58
2003	5,502	8	712 \pm 80
2004	7,971	14	591 \pm 47
2005	13,245	14	1010 \pm 81
2006	13,986	38	656 \pm 45
2007	3,400	3	512 \pm 142
2008	3,990	1	1133
2009	9,393	34	799 \pm 44
All	69,481	139	749 \pm 24
Jan–Apr	19,994	33	838 \pm 54
May–Nov	49,487	106	726 \pm 26

^a“Dry” years were 2002, 2004, 2006, and 2009. “Wet” years were 2001, 2003, 2005, 2007, and 2008.

^bFire counts are the total observed MODIS CMG annual fire counts for each island.

^cMeans were constructed by first estimating the mean height of all the individual retrievals within a single plume, and then by constructing a mean of all the plumes in a given year or set of years. SE (standard error) was computed as (σ/\sqrt{n}) where n = number of plumes.

determined by the user (M. Tosca) and were often defined as the point where smoke was no longer opaque enough to allow for a successful height retrieval from MINX. The mean cross-sectional height (above terrain) of all Borneo smoke retrievals was fairly uniform, with smoke reaching a mean height of 600–900 m for the vast majority of pixels within \sim 50 km of the origin (Figures 10 and S10). Mean smoke heights were somewhat lower for retrievals further than \sim 70 km from the origin.

4. Discussion

[38] Direct injection of fire emissions into the middle to upper troposphere within fire plumes did not appear to be an important mechanism for vertical mixing of aerosols in equatorial Asia during our study period. Mean plume heights were 709 \pm 14 m on Borneo and 749 \pm 24 m on Sumatra and were similar to the median plume height estimates for tropical and temperate forest regions reported by *Val Martin et al.* [2010] (744 and 781 m, respectively). Only 4% of plumes in our study had heights that were more than 500 m above the ABL; these levels were near or at the lower bound of the percentage of plumes observed above the ABL by *Val Martin et al.* [2010]. Many fires in this region occurred in peat forests (e.g., Figure 1) and therefore would be

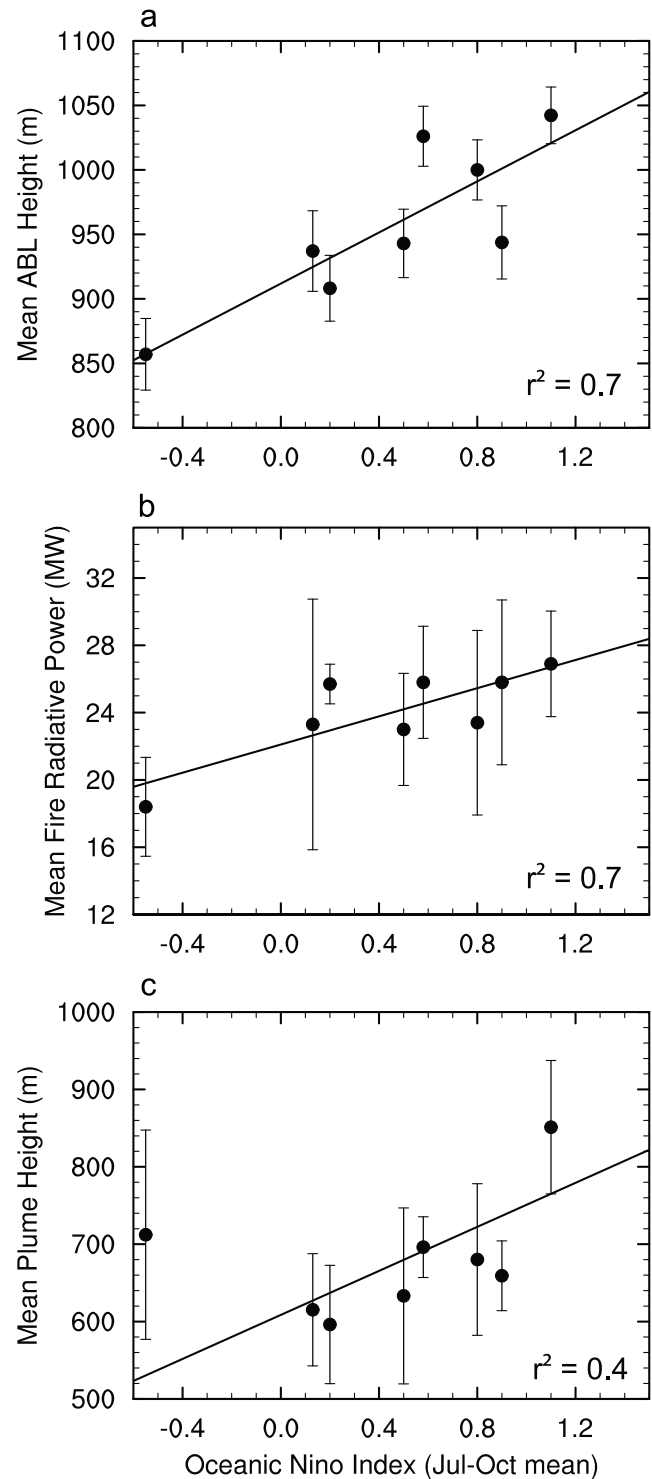


Figure 6. For Borneo, the relationship between (a) Oceanic Niño Index (ONI) and the mean atmospheric boundary layer (ABL) ($r^2 = 0.7$, $p < 0.01$), (b) ONI and mean fire radiative power ($r^2 = 0.7$, $p < 0.01$), and (c) ONI and mean plume height ($r^2 = 0.4$, $p = 0.04$). For ONI we used the June–December mean ONI ($\Delta^\circ\text{C}$) as an indicator of El Niño strength. The mean ABL and plume heights are reported in units of meters above terrain. The regression in Figure 6c is weighted by the number of plumes observed each year.

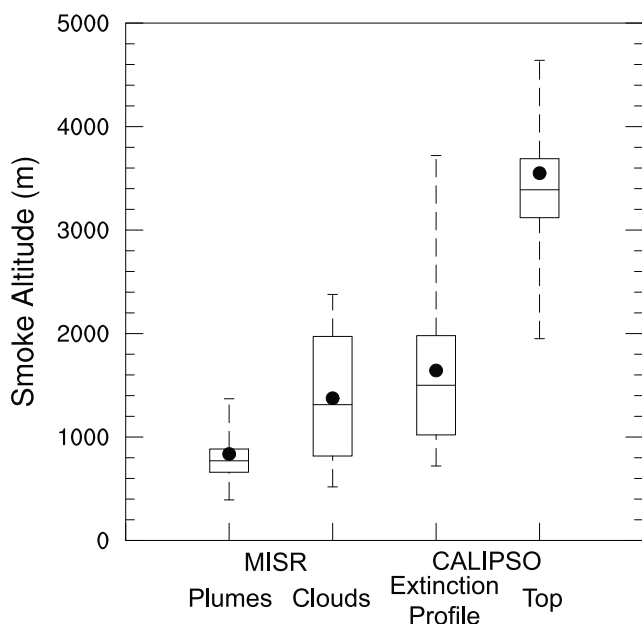


Figure 7. Comparison of distributions of individual smoke plume altitudes and smoke cloud altitudes on Borneo (from both MISR and CALIPSO) during 26 September to 1 November 2006. The top and bottom of each box indicate the 66th and 33rd percentiles, respectively. The top and bottom whisker lines indicate the 95th and 5th percentiles, respectively. The central line indicates the median, and the dot represents the mean. “CALIPSO extinction” refers to the mean vertical distribution of aerosol extinction for nighttime scenes from 26 September to 1 November 2006. “CALIPSO top” data is the Level 2 product estimate of smoke top altitudes for all nighttime smoke retrievals over the same period.

expected to have relatively low fire intensities [Page *et al.*, 2002; van der Werf *et al.*, 2008]. The relatively low injection heights of fire plumes observed in this study were consistent with the smoldering nature expected for many peat fires [Duncan *et al.*, 2003], and are unlike those of the large boreal crown fire plumes of Alaska, or the higher-intensity grass fires of Australia [e.g., Kahn *et al.*, 2008; Mims *et al.*, 2010].

[39] On Borneo, and to a lesser extent on Sumatra, fire and smoke occurrence were linked with El Niño. During periods of El Niño-induced drought (2002, 2004, 2006, and 2009), we observed substantially higher numbers of MODIS active fires, MISR-derived smoke plumes, and (2006–2009) CALIPSO-derived observations of smoke clouds. Over 80% of all MISR smoke plumes observed on Borneo occurred during El Niño years. The horizontal fractional coverage of smoke in the CALIPSO time series rarely exceeded 0.20, except during the El Niño periods of the fall of 2006 and 2009. These results are consistent with both the van der Werf *et al.* [2008] and Field *et al.* [2009] studies that quantitatively link fire emissions and El Niño in equatorial Asia.

[40] In addition to increasing the number of observed fires (and plumes), El Niño influenced plume heights. The mean annual plume height on Borneo during El Niño years was

significantly higher than that for non-El Niño years. The association between ONI and both ABL height and mean FRP may partly explain the link between El Niño strength and injection height. Observations of monthly ABL were strongly correlated with ONI on Borneo (Figure S3). In contrast, no correlation between plume heights and ONI was observed on Sumatra. Field *et al.* [2009] summarize the predictability of ENSO (among other climate variables) in determining carbon emissions in Indonesia and conclude that ENSO has less predictive ability for Sumatra fire emissions than for Borneo fire emissions. Their work provides evidence that fire patterns are controlled by other climate processes (including the Indo-Australian monsoon) and may explain why we did not observe a correlation between plume heights and ENSO on Sumatra.

[41] Observed smoke cloud altitudes on Borneo (from fall 2006) were higher than plume altitudes, but still showed the majority of smoke residing between 1000 and 2000 m above sea level. The median altitude of all cloud height retrievals from MISR during the fall of 2006 was over 500 m higher than the median altitude of all individual plume height retrievals. CALIPSO measurements for 2006–2009 showed dense smoke at similar altitudes, with very little extinction by smoke aerosols at altitudes above 3500 m. The difference in height between smoke plumes and clouds may be partially explained by the diurnal evolution of the ABL in this region. Schafer *et al.* [2001] observed a relatively shallow early morning ABL expanding throughout the day in tandem with increased insolation, reaching its maximum in the afternoon, and collapsing overnight. MERRA data (not shown) during the fire season showed that the ABL expanded during late morning, reaching a peak altitude in the early afternoon that was 100–200 m higher than the overnight minimum. Thus, plumes detected by MISR in the morning were likely injected into a relatively shallow ABL. If these same fires persisted throughout the day, smoke that remained in the ABL may have risen with the vertical expansion of the ABL in the afternoon and then remained

Table 3. Summary of 2006 Smoke Cloud Data

Date	Area (km ²)	Longitude ^a (°E)	Latitude ^a (°N)	Mean Altitude ± SD (m)
26 Sep 2006	21,345	113.9	-2.0	1192 ± 432
1 Oct 2006	39,582	109.7	0.9	1184 ± 769
5 Oct 2006	120,332	114.2	-0.6	1088 ± 597
8 Oct 2006	16,026	108.1	-0.9	1064 ± 431
12 Oct 2006	95,869	113.4	-1.1	1795 ± 456
17 Oct 2006	58,888	108.6	-1.3	1108 ± 494
19 Oct 2006	52,709	111.8	-0.6	1517 ± 588
21 Oct 2006	23,291	113.9	-2.6	1359 ± 528
28 Oct 2006	23,323	113.9	-2.0	1230 ± 479
30 Oct 2006	71,232	115.6	-0.5	1518 ± 641
All	522,597	112.9	-0.9	1375 ± 608
Ocean ^b	114,496	109.0	-0.5	1127 ± 588
Land ^c	408,101	113.9	-1.0	1441 ± 613

^aLatitude and longitude values are the mean latitude and mean longitude of all valid smoke retrievals.

^bOcean clouds consisted of smoke that was primarily observed over the ocean between Borneo and Sumatra (1 October 2006, 8 October 2006, and 17 October 2006).

^cLand clouds were primarily observed over the landmass of Borneo (26 September 2006, 5 October 2006, 12 October 2006, 19 October 2006, 21 October 2006, 28 October 2006, and 30 October 2006).

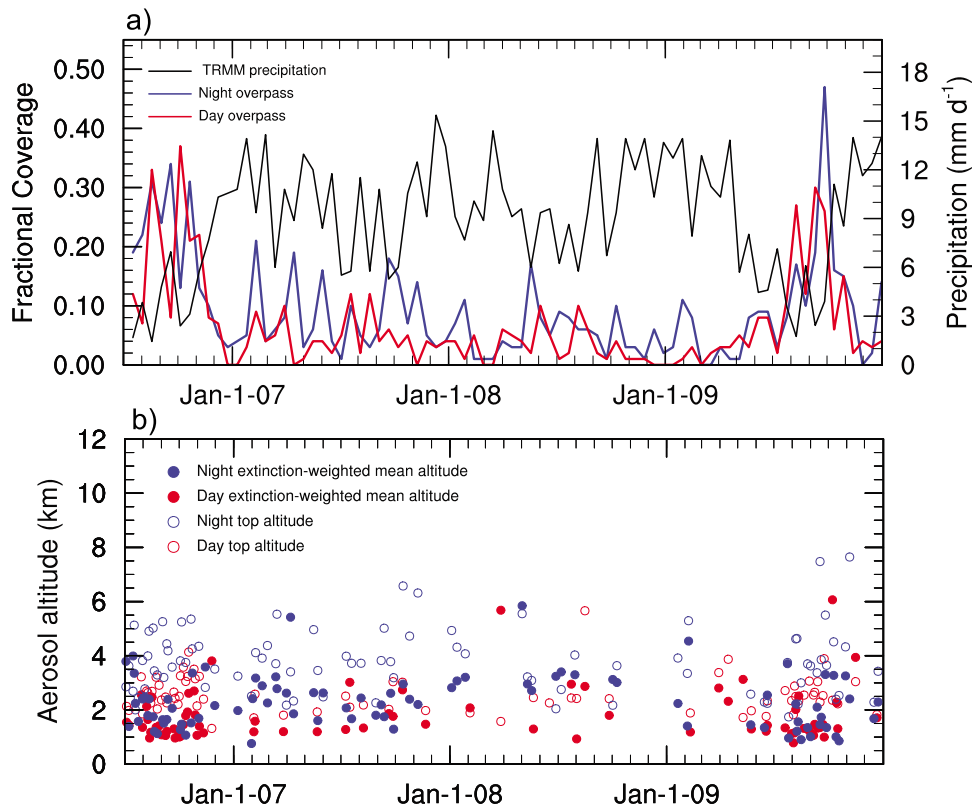


Figure 8. CALIPSO observations of fractional smoke cover and altitudes during 2006–2009 over Borneo (3°S–3°N, 110°E–117°E). (a) The 16 day mean horizontal fractional coverage of smoke in each CALIPSO overpass (blue line is night overpass, and red line is day overpass) compared with 16 day mean precipitation (mm d⁻¹) from TRMM (black line). (b) The mean smoke top altitudes (open circles) and extinction-weighted mean altitudes (solid circles) for each CALIPSO overpass containing >15% horizontal smoke coverage (night is indicated by blue, and day is indicated by red).

aloft over night. Convection over land also reaches a maximum during the afternoon [Mori *et al.*, 2004] and is another mechanism by which low-level smoke may be transported aloft. Over a period of multiple days, these mechanisms may

lead to clouds that are significantly higher than their younger plume counterparts. However, there was no evidence for deep injection of smoke into the troposphere in either smoke plumes or smoke clouds.

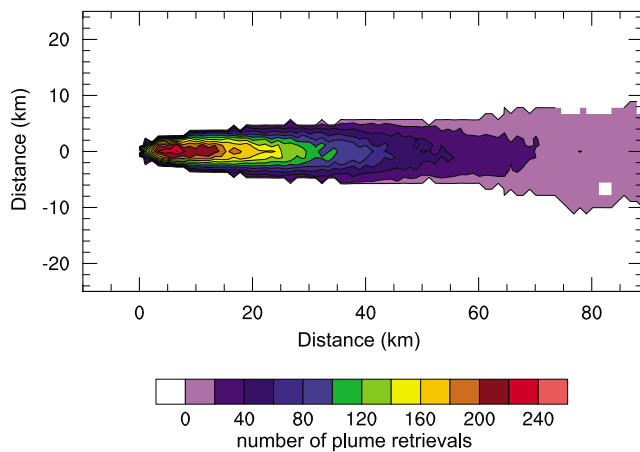


Figure 9. Density distribution of plume stereoheight retrievals on Borneo after normalizing each plume perimeter to a common origin and aligning all plumes along their origin-to-centroid axis. Only retrievals within 2 standard deviations (km) of the origin-centroid axis are shown.

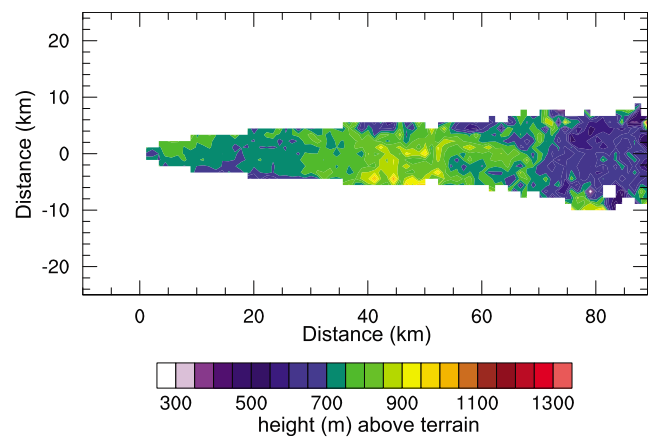


Figure 10. Mean smoke plume heights on Borneo where more than one plume retrieval was recorded after normalizing each plume perimeter to a common origin and aligning all plumes along their origin-to-centroid axis (similar to Figure 9).

[42] Nearly all observed plumes drifted from southeast to northwest (Figure S8), an observation that likely explained the presence of smoke clouds over central Borneo (Figure S5). These observations and the spatial pattern of smoke clouds over Borneo suggest that the transport of young smoke from fires burning in southeastern Borneo was partly blocked by the central island mountain range. Smoke that collected on the southeastern edge of this range may have been subjected to the diurnal ABL expansion described above. This trapping and mixing may have increased the persistence of horizontal and vertically expansive smoke clouds over central and southern Borneo. Not only were smoke clouds higher, but they covered substantially more horizontal area than smoke plumes. The area of all plumes on Borneo and Sumatra observed during 2001–2009 was approximately one quarter the size of Borneo. Plumes during 2006 accounted for approximately 19% of the total area of all plumes but this coverage was considerably smaller than for smoke clouds. More specifically, the total area for 2006 smoke clouds was nearly 25 times larger than the area of concurrent smoke plumes, highlighting the overall importance of smoke clouds for atmospheric chemistry, air quality and climate. The August–October 2006 mean fractional coverage of smoke for nighttime CALIPSO overpasses was 0.3. Extrapolating this figure to the entire island of Borneo suggests that smoke covered a horizontal area similar to the total smoke cloud area derived from MINX. *Tosca et al.* [2010] present aerosol optical depth (AOD) observations from MISR showing high AODs extending well to the west of Borneo and Sumatra during El Niño years and suggesting that the horizontal extent of smoke clouds presented here is a lower bound estimate.

5. Conclusions

[43] Understanding plume injection dynamics and their life cycle evolution to more expansive smoke clouds is an important aspect of better quantifying the climate impact of fire-emitted aerosols. Several recent studies [e.g., *Duncan et al.*, 2003; *Podgorny et al.*, 2003; *Tosca et al.*, 2010] highlight the need to improve our ability to quantify the impact of Indonesian smoke on surface and atmospheric radiation budgets of the region. High-resolution MISR aerosol optical depth data from the El Niño years of 2002, 2004 and 2006 indicate smoke covered an area from Papua New Guinea to the central Indian Ocean and from northern Australia to southern Thailand. Here we quantified the height and altitude of this smoke, considering both plumes and clouds.

[44] Plumes were generally confined to altitudes below 1000 m, whereas examination of smoke clouds indicated smoke commonly residing between 1000 and 2000 m above sea level. The majority of plumes in Indonesia drifted toward the northwest and originated in peat forests. Most plumes did not extend above the ABL, suggesting that the top of the ABL was a good proxy for the maximum height of aerosol plumes. We also found that ENSO had a strong effect on both plume number and the aerial extent of smoke clouds, particularly on the island of Borneo.

[45] There was good agreement between MISR smoke cloud altitudes and the CALIPSO extinction-weighted mean smoke altitudes. The benefits of using MISR data included

increased spatial and temporal coverage (with imagery extending back to 2000), as well as the ability to view the actual injection region for individual plumes. In contrast, though CALIPSO rarely observed the actual fire source, its data products provided more detailed information about smoke and aerosol vertical distribution. Due to its sensitivity to thin aerosol layers, CALIPSO was able to quantify the existence of thin smoke layers in the midtroposphere above Borneo, between 2000 and 4500 m.

[46] Observations from both instruments provide a means to improve the representation of fire-emitted aerosols within climate models. Ultimately this information may improve our ability to understand interactions between El Niño, the terrestrial carbon cycle, and atmospheric chemistry in the region and thus the means to develop more realistic scenarios of climate change during the 21st century. Important next steps are to quantify the mesoscale processes and island-ocean interactions that regulate smoke cloud formation and dissipation and the mechanisms by which relatively low smoke plumes evolve into relatively high smoke clouds.

[47] **Acknowledgments.** The data presented here are publicly available in a database of plume injection heights (<http://misr.jpl.nasa.gov/getData/accessData/MisrMinxPlumes/>). We thank three anonymous reviewers for critical analysis and insightful comments about the interpretation of our results. We thank Ralph Kahn for advice on comparisons between MISR and CALIPSO altitudes. We are grateful for support from NSF (ATM-0628637) and NASA (NNX08AF64G). M.G.T. received support from a NASA Earth and Space Science Fellowship (08-Earth08F-189). C.S.Z. acknowledges NSF (ARC-0714088) and NASA (NNX07AR23G) support. The MINX plume digitizing tool is publicly available for Apple and PC users and can be downloaded at: <http://www.openchannelfoundation.org/projects/MINX>.

References

- Aiken, S. R. (2004), Runaway fires, smoke-haze pollution, and unnatural disasters in Indonesia, *Geogr. Rev.*, *94*, 55–79, doi:10.1111/j.1931-0846.2004.tb00158.x.
- Andreae, M. O., and P. Merlet (2001), Emission of trace gases and aerosols from biomass burning, *Global Biogeochem. Cycles*, *15*, 955–966, doi:10.1029/2000GB001382.
- Andreae, M. O., P. Artaxo, H. Fischer, S. R. Freitas, J. M. Gregoire, A. Hansel, P. Hoor, R. Kormann, R. Krejci, and L. Lange (2001), Transport of biomass burning smoke to the upper troposphere by deep convection in the equatorial region, *Geophys. Res. Lett.*, *28*, 951–954, doi:10.1029/2000GL012391.
- Boden, T. A., G. Marland, and R. J. Andres (2010), *Global, Regional, and National Fossil-Fuel CO₂ Emissions*, Carbon Dioxide Inf. Anal. Cent., Oak Ridge Natl. Lab., U.S. Dep. of Energy, Oak Ridge, Tenn.
- Bosilovich, M., J. Chen, F. R. Robertson, and R. F. Adler (2008), Evaluation of global precipitation in reanalyses, *J. Appl. Meteorol. Climatol.*, *47*, 2279–2299, doi:10.1175/2008JAMC1921.1.
- Chen, Y., Q. Li, J. T. Randerson, E. A. Lyons, R. A. Kahn, D. L. Nelson, and D. J. Diner (2009), The sensitivity of CO and aerosol transport to the temporal and vertical distribution of North American boreal fire emissions, *Atmos. Chem. Phys.*, *9*, 6559–6580, doi:10.5194/acp-9-6559-2009.
- Colarco, P. R., M. R. Schoeberl, B. G. Doddridge, L. T. Marufu, O. Torres, and E. J. Welton (2004), Transport of smoke from Canadian forest fires to the surface near Washington, DC: Injection height, entrainment, and optical properties, *J. Geophys. Res.*, *109*, D06203, doi:10.1029/2003JD004248.
- Davies, S. J., and L. Unam (1999), Smoke-haze from the 1997 Indonesian forest fires: Effects on pollution levels, local climate, atmospheric CO₂ concentrations, and tree photosynthesis, *For. Ecol. Manage.*, *124*, 137–144, doi:10.1016/S0378-1127(99)00060-2.
- Diner, D. J., J. C. Beckert, T. H. Reilly, C. J. Bruegge, J. E. Conel, R. A. Kahn, J. V. Martonchik, T. P. Ackerman, R. Davies, and S. A. W. Gerstl (1998), Multi-angle Imaging Spectroradiometer (MISR) instrument description and experiment overview, *IEEE Trans. Geosci. Remote Sens.*, *36*, 1072–1087, doi:10.1109/36.700992.

- Duncan, B. N., I. Bey, M. Chin, L. J. Mickley, T. D. Fairlie, R. V. Martin, and H. Matsueda (2003), Indonesian wildfires of 1997: Impact on tropospheric chemistry, *J. Geophys. Res.*, *108*(D15), 4458, doi:10.1029/2002JD003195.
- Emmanuel, S. C. (2000), Impact to lung health of haze from forest fires: The Singapore experience, *Respirology*, *5*, 175–182, doi:10.1046/j.1440-1843.2000.00247.x.
- Field, R. D., G. R. van der Werf, and S. S. P. Shen (2009), Human amplification of drought-induced biomass burning in Indonesia since 1960, *Nat. Geosci.*, *2*, 185–188, doi:10.1038/ngeo443.
- Freitas, S. R., K. M. Longo, and M. O. Andreae (2006), Impact of including the plume rise of vegetation fires in numerical simulations of associated atmospheric pollutants, *Geophys. Res. Lett.*, *33*, L17808, doi:10.1029/2006GL026608.
- Fromm, M. D., and R. Servranckx (2003), Transport of forest fire smoke above the tropopause by supercell convection, *Geophys. Res. Lett.*, *30*(10), 1542, doi:10.1029/2002GL016820.
- Giglio, L., I. Csizsar, and C. O. Justice (2006), Global distribution and seasonality of active fires as observed with the Terra and Aqua Moderate Resolution Imaging Spectroradiometer (MODIS) sensors, *J. Geophys. Res.*, *111*, G02016, doi:10.1029/2005JG000142.
- Hastings, D. A., et al. (Eds.) (1999), The Global Land One-kilometer Base Elevation (GLOBE) digital elevation model, version 1.0, <http://www.ngdc.noaa.gov/mgg/topo/globe.html>, Natl. Geophys. Data Cent., NOAA, Boulder, Colo.
- Kahn, R. A., W. H. Li, C. Moroney, D. J. Diner, J. V. Martonchik, and E. Fishbein (2007), Aerosol source plume physical characteristics from space-based multiangle imaging, *J. Geophys. Res.*, *112*, D11205, doi:10.1029/2006JD007647.
- Kahn, R. A., Y. Chen, D. L. Nelson, F. Y. Leung, Q. Li, D. J. Diner, and J. A. Logan (2008), Wildfire smoke injection heights: Two perspectives from space, *Geophys. Res. Lett.*, *35*, L04809, doi:10.1029/2007GL032165.
- Kummerow, C., W. Barnes, T. Kozu, J. Shiue, and J. Simpson (1998), The tropical rainfall measuring mission (TRMM) sensor package, *J. Atmos. Oceanic Technol.*, *15*, 809–817, doi:10.1175/1520-0426(1998)015<0809:TTRMMT>2.0.CO;2.
- Labonne, M., F. M. Bréon, and F. Chevallier (2007), Injection height of biomass burning aerosols as seen from a spaceborne lidar, *Geophys. Res. Lett.*, *34*, L11806, doi:10.1029/2007GL029311.
- Leung, F. Y. T., J. A. Logan, R. Park, E. Hyer, E. Kasischke, D. Streets, and L. Yurganov (2007), Impacts of enhanced biomass burning in the boreal forests in 1998 on tropospheric chemistry and the sensitivity of model results to the injection height of emissions, *J. Geophys. Res.*, *112*, D10313, doi:10.1029/2006JD008132.
- Logan, J. A., I. Megretskaja, R. Nassar, L. T. Murray, L. Zhang, K. W. Bowman, H. M. Worden, and M. Luo (2008), Effects of the 2006 El Niño on tropospheric composition as revealed by data from the Tropospheric Emission Spectrometer (TES), *Geophys. Res. Lett.*, *35*, L03816, doi:10.1029/2007GL031698.
- Marland, G., T. A. Boden, R. J. Andres, A. L. Brenkert, and C. A. Johnston (2006), Global, regional, and national fossil fuel CO₂ emissions, in *Trends: A Compendium of Data on Global Change* [electronic], doi:10.3334/CDIAC/00001, Carbon Dioxide Inf. Anal. Cent., Oak Ridge Natl. Lab., U.S. Dep. of Energy, Oak Ridge, Tenn.
- Mims, S. R., R. A. Kahn, C. M. Moroney, B. J. Gaitley, D. L. Nelson, and M. J. Garay (2010), MISR stereo heights of grassland fire smoke plumes in Australia, *IEEE Trans. Geosci. Remote Sens.*, *48*, 25–35.
- Mori, S., H. Jun-Ichi, Y. I. Tauhid, M. D. Yamanaka, N. Okamoto, F. Murata, N. Sakurai, H. Hashiguchi, and T. Sribimawati (2004), Diurnal land–sea rainfall peak migration over Sumatera Island, Indonesian maritime continent, observed by TRMM satellite and intensive rawinsonde soundings, *Mon. Weather Rev.*, *132*, 2021–2039, doi:10.1175/1520-0493(2004)132<2021:DLRPMO>2.0.CO;2.
- Murdiyarso, D., and E. S. Adiningsih (2007), Climate anomalies, Indonesian vegetation fires and terrestrial carbon emissions, *Mitigation Adapt. Strategies Global Change*, *12*, 101–112, doi:10.1007/s11027-006-9047-4.
- Nelson, D. L., C. Averill, S. Boland, R. Morford, M. Garay, C. Thompson, J. Hall, D. Diner, and H. Campbell (2008a), MISR Interactive Explorer (MINX) v1.0 user's guide, NASA Jet Propul. Lab., Pasadena, Calif. (Available at <http://www.openchannelsoftware.com/projects/MINX>.)
- Nelson, D. L., Y. Chen, R. A. Kahn, D. J. Diner, and D. Mazzoni (2008b), Example applications of the MISR Interactive Explorer (MINX) software tool to wildfire smoke plume analyses, *Proc. SPIE*, *7089*, 708909.1–708909.11.
- Olson, D. M., et al. (2001), Terrestrial ecoregions of the world: A new map of life on Earth, *BioScience*, *51*, 933–938, doi:10.1641/0006-3568(2001)051[0933:TEOTWA]2.0.CO;2.
- Omar, A. H., D. M. Winker, C. Kittaka, M. A. Vaughan, Z. Liu, Y. Hu, C. R. Trepte, R. R. Rogers, R. A. Ferrare, and K. P. Lee (2009), The CALIPSO automated aerosol classification and lidar ratio selection algorithm, *J. Atmos. Oceanic Technol.*, *26*, 1994–2014, doi:10.1175/2009JTECHA1231.1.
- Ott, L., B. Duncan, S. Pawson, P. Colarco, M. Chin, C. Randles, T. Diehl, and E. Nielsen (2010), Influence of the 2006 Indonesian biomass burning aerosols on tropical dynamics studied with the GEOS-5 AGCM, *J. Geophys. Res.*, *115*, D14121, doi:10.1029/2009JD013181.
- Page, S. E., F. Siebert, J. O. Rieley, H. V. Boehm, A. Jaya, and S. Limin (2002), The amount of carbon released from peat and forest fires in Indonesia during 1997, *Nature*, *420*, 61–65, doi:10.1038/nature01131.
- Podgorny, I. A., F. Li, and V. Ramanathan (2003), Large aerosol radiative forcing due to the 1997 Indonesian forest fire, *Geophys. Res. Lett.*, *30*(1), 1028, doi:10.1029/2002GL015979.
- Schafer, R., P. T. May, T. D. Keenan, K. McGuffie, W. L. Ecklund, P. E. Johnson, and K. S. Gage (2001), Boundary layer development over a tropical island during the Maritime Continent Thunderstorm Experiment, *J. Atmos. Sci.*, *58*, 2163–2179.
- Sodhi, N. S., L. P. Koh, B. W. Brook, and P. K. L. Ng (2004), Southeast Asian biodiversity: An impending disaster, *Trends Ecol. Evol.*, *19*, 654–660, doi:10.1016/j.tree.2004.09.006.
- Thompson, A. M., J. C. Witte, R. D. Hudson, H. Guo, J. R. Herman, and M. Fujiwara (2001), Tropical tropospheric ozone and biomass burning, *Science*, *291*, 2128–2132, doi:10.1126/science.291.5511.2128.
- Tosca, M. G., J. T. Randerson, C. S. Zender, M. G. Flanner, and P. J. Rasch (2010), Do biomass burning aerosols intensify drought in equatorial Asia during El Niño?, *Atmos. Chem. Phys.*, *10*, 3515–3528, doi:10.5194/acp-10-3515-2010.
- Trenberth, K. E. (1997), The definition of El Niño, *Bull. Am. Meteorol. Soc.*, *78*, 2771–2777, doi:10.1175/1520-0477(1997)078<2771:TDOE-NO>2.0.CO;2.
- Val Martin, M. V., J. A. Logan, R. A. Kahn, F. Y. Leung, D. L. Nelson, and D. J. Diner (2010), Smoke injection heights from fires in North America: Analysis of 5 years of satellite observations, *Atmos. Chem. Phys.*, *10*, 1491–1510, doi:10.5194/acp-10-1491-2010.
- van der Werf, G. R., J. T. Randerson, L. Giglio, G. J. Collatz, P. S. Kasibhatla, and A. F. Arellano Jr. (2006), Interannual variability of global biomass burning emissions from 1997 to 2004, *Atmos. Chem. Phys.*, *6*, 3423–3441, doi:10.5194/acp-6-3423-2006.
- van der Werf, G. R., J. Dempewolf, S. N. Trigg, J. T. Randerson, P. S. Kasibhatla, L. Giglio, D. Murdiyarso, W. Peters, D. C. Morton, and G. J. Collatz (2008), Climate regulation of fire emissions and deforestation in equatorial Asia, *Proc. Natl. Acad. Sci. U. S. A.*, *105*, 20,350–20,355, doi:10.1073/pnas.0803375105.
- Vaughan, M. A., D. M. Winker, and K. A. Powell (2005), CALIOP algorithm theoretical basis document, part 2: Feature detection and layer properties algorithms, *Rep. PC-SCI-202.01*, NASA Langley Res. Cent., Hampton, Va.
- Westphal, D. L., and O. B. Toon (1991), Simulations of microphysical, radiative, and dynamical processes in a continental-scale forest fire smoke plume, *J. Geophys. Res.*, *96*, 22,379–22,400, doi:10.1029/91JD01956.
- Wikramanayake, E., E. Dinerstein, C. Loucks, D. Olson, J. Morrison, J. Lamoreux, M. McKnight, and P. Hedao (2001), *Terrestrial Ecoregions of the Indo-Pacific: A Conservation Assessment*, Island, Washington, D. C.
- Yang, Z., R. A. Washenfelder, G. Keppel-Aleks, N. Y. Krakauer, J. T. Randerson, P. P. Tans, C. Sweeney, and P. O. Wennberg (2007), New constraints on Northern Hemisphere growing season net flux, *Geophys. Res. Lett.*, *34*, L12807, doi:10.1029/2007GL029742.
- Young, S. A., and M. A. Vaughan (2009), The retrieval of profiles of particulate extinction from Cloud-Aerosol Lidar Infrared Pathfinder Satellite Observations (CALIPSO) data: Algorithm description, *J. Atmos. Oceanic Technol.*, *26*, 1105–1119, doi:10.1175/2008JTECHA1221.1.

D. J. Diner and D. L. Nelson, Jet Propulsion Laboratory, California Institute of Technology, Pasadena, CA 91109, USA.

J. A. Logan, School of Engineering and Applied Science, Harvard University, Cambridge, MA 02138, USA.

J. T. Randerson, M. G. Tosca, and C. S. Zender, Department of Earth System Science, University of California, Irvine, CA 92697, USA. (mtosca@uci.edu)